JTE
HCMUTE
ISSN: 2615-9740

JOURNAL OF TECHNICAL EDUCATION SCIENCE
Ho Chi Minh City University of Technology and Education
Website: https://jte.hcmute.edu.vn/index.php/jte/index
Email: jte@hcmute.edu.vn

Dynamic Analysis and Isolation Effectiveness of a Low Stiffness Nonlinear Isolator

Nguyen Minh Ky[1], Vo Ngoc Yen Phuong[1,2], Le Thanh Danh[2*]

[1]*Ho Chi Minh City University of Technology and Education, Vietnam*
[2]*Industrial University of Ho Chi Minh City, Vietnam*

[*] Corresponding author. *Email: lethanhdanh@iuh.edu.vn*

ARTICLE INFO

Received: 01/07/2022
Revised: 12/08/2022
Accepted: 18/08/2022
Published: 28/10/2022

KEYWORDS

Pneumatic cylinder;
Auxiliary chamber;
Low dynamic stiffness;
Nonlinear vibration isolator;
Low Frequency isolation.

ABSTRACT

This paper presents a low stiffness nonlinear vibration isolator using a pneumatic spring with an auxiliary chamber which is shortened by LSNVI. Firstly, the mechanical model of the isolator, which is constructed by two opposite stiffness mechanisms includes the load bearing mechanism (LBM) and the stiffness corrected mechanism (SCM), is introduced. Secondly, the restoring force of the model is found. Based on this, the dynamic stiffness is calculated numerically. Then, the spring force curve was approximated by expanding the Taylor series to order-5. Next, a numerical simulation is carried out to investigate the effect of the pressure ratio on the system stiffness. Simultaneously, by using the Multi-scale method, the frequency-amplitude relation curve is analyzed. The vibration transmissibility characteristic of the LSNVI is simulated and compared with that of the equivalent traditional nonlinear vibration isolator (named NVI-non SCM) in which the SCM is removed. The simulation results illustrate that the isolation effectiveness of the former is better than the latter. This result shows that the LSNVI can offer a vision isolation performance. This presentation furnishes a useful insight into the design for low frequency vibration isolation model

Doi: https://doi.org/10.54644/jte.72A.2022.1243

1. Introduction

In engineering, vibration is one of the reasons which can cause damage or unstable to machinery, equipment, etc. In order to ensure equipment works accurately as well as improve its long life. Isolators are useful indeed, especially the isolator with variable stiffness is deeply paid attention of science community. Firstly, isolators with coil or rubber springs whose stiffness is constant [1-2] which has a low load supporting capacity. In the same manner, isolators using Euler springs, which provide the low stiffness [3-4]. Another problem of an isolator with constant stiffness that is too difficult to overcome is that the stiffness can not be easily adjusted as the isolated load changes. In recent years, the magnetic springs [5-8] have been studied commonly for vibration isolation. Besides, with a variable in stiffness, these magnetic elastic elements can be simply controlled to upgrade the effectiveness of isolation such as some studies of G. Dong et al. [9] – [10].

As an alternative, the isolation models using air springs are used widely in engineering practice. M.W. Holtz et al. [11] analyzed theoretically and investigated experimentally a suspension seat using air springs. The air spring force is controlled to improve the isolation performance of the seat suspension system as studied by I. Maciejewski et al. [12] – [13]. M.M. Moheyeldein et al. [14] investigated the dynamic response of the air spring suspensions, providing more comfortable and convenient handling performances than the passive suspension. In addition, a position controller for the seat suspension using air springs was proposed and carried out experimentally by I. Maciejewski et al. [15]. Besides, Tran X.B. et al. proposed a set of two Pneumatic Linear Actuators [16] added to a seat supported by a pneumatic spring which makes the seat more comfortable. This work shows the advantages of using pneumatic spring in a driver seat by adjusting the pressure of the pneumatic spring. Nguyen et al. [17] introduced a new vibration which is composed by two air bellow elements

JTE
HCMUTE
ISSN: 2615-9740

JOURNAL OF TECHNICAL EDUCATION SCIENCE
Ho Chi Minh City University of Technology and Education
Website: https://jte.hcmute.edu.vn/index.php/jte/index
Email: jte@hcmute.edu.vn

in horizontal direction in perpendicular to a sleeve -type air spring element. This work can improve the comfort of vehicle seats since decreasing in seat displacement and enlarging the isolation effectiveness under low excitation frequency is excellent. Vo et al. [18] proposed and performed the static analysis of a low frequency vibration isolation model, indicating that the dynamic stiffness of the proposed model can be adjusted to obtain an expected low stiffness.

In order to extend our study relating to works presented in [18], the main purpose of this paper is to analyze the dynamic response as well as isolation effectiveness of the low stiffness nonlinear vibration isolator using a pneumatic spring with an auxiliary chamber. First of all, the mechanical model of the LSNVI and its dynamic stiffness will be presented. Then, the dynamic response of the LSNVI is analyzed by using the Multi-scale method. From this result, the transmissibility of vibration will be attained. In addition, the effectiveness performance of the LSNVI is drawn and also compared the NVI non SCM through the numerical simulation.

2. Nonlinear vibration isolation model

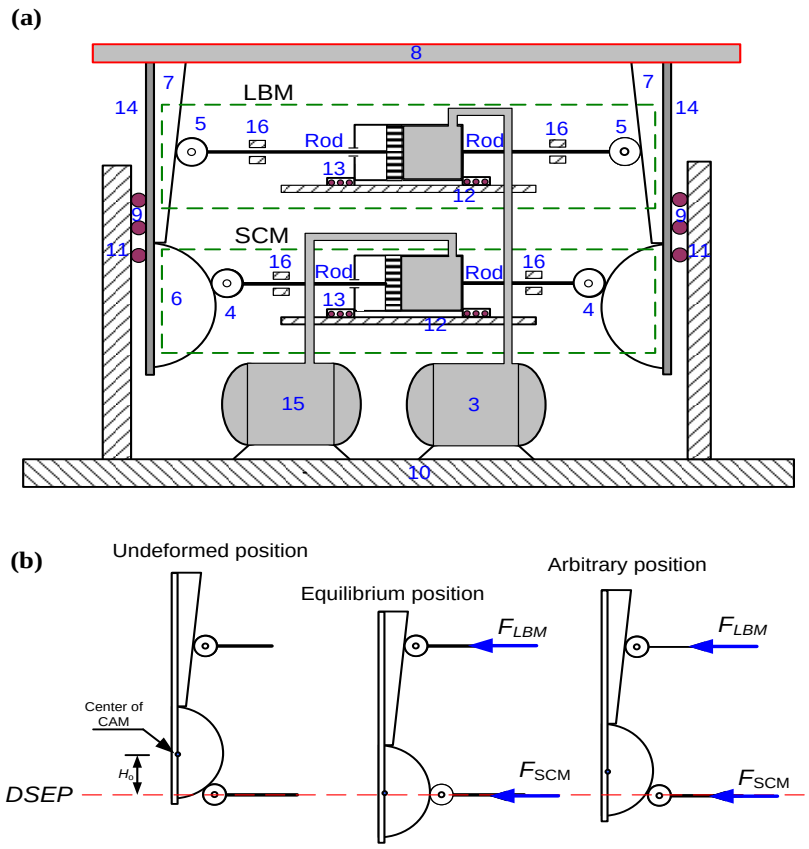

Figure.1. (a) *Schematic diagram of LSNVI; (b) Specific working states*

As introduced in [18], the principle of the nonlinear vibration isolation model is shown in Fig. 1. In which two semicircular cams (6) and two wedges (7) are fixed on the legs (14) meanwhile these legs are also fixed on the load plate (8) and only moves vertically through rollers (9) and the guide-bars (11). In terms of mechanism, all private parts are considered as one solid. Especially, the pneumatic cylinders work as restoring elements. This model can be divided into two mechanisms. One with positive stiffness comprising wedges, rollers (5), pneumatic cylinder (13) and auxiliary tank (3) is used to support the load. The feature of this mechanism has the positive stiffness in vertical direction, which is used to bear load named “LBM”. The other offers the vertical negative stiffness including semicircular cams (6), rollers (4), pneumatic cylinder (13) and auxiliary tank (15). It is called the stiffness corrected mechanism “SCM” which is used to correct the system stiffness. During operation, rollers always roll without on the surface of the cam and the wedge, simultaneously, the center of the rollers only moves in horizontal direction via the linear busing (16). While, the cylinders will slide on the horizontal guide-bars (14) thank to the linear busing (13)

JTE HCMUTE
ISSN: 2615-9740
JOURNAL OF TECHNICAL EDUCATION SCIENCE
Ho Chi Minh City University of Technology and Education
Website: https://jte.hcmute.edu.vn/index.php/jte/index
Email: jte@hcmute.edu.vn

When the system is working, it can appear three positions such as undeformed, static equilibrium and arbitrary position. At the first one, the cylinders are not compressed. The second position is defined at which the centers of the cam (6) and roller (4) are the same horizontal line denoted by the red dash line as in Fig. 1(b), which is defined as the design static equilibrium position (shortened DSEP).

3. Dynamic equation

A simple model of the LSNVI is presented in Fig. 2. Where, the isolated object consists of the wedges, semicircular cam, legs, load plate and the object placed on the load plate. The weight of the isolated object is the total weight of these objects. Supposing that the isolated object is displaced vertically *y*, due to the base displacement excitation, z_e,

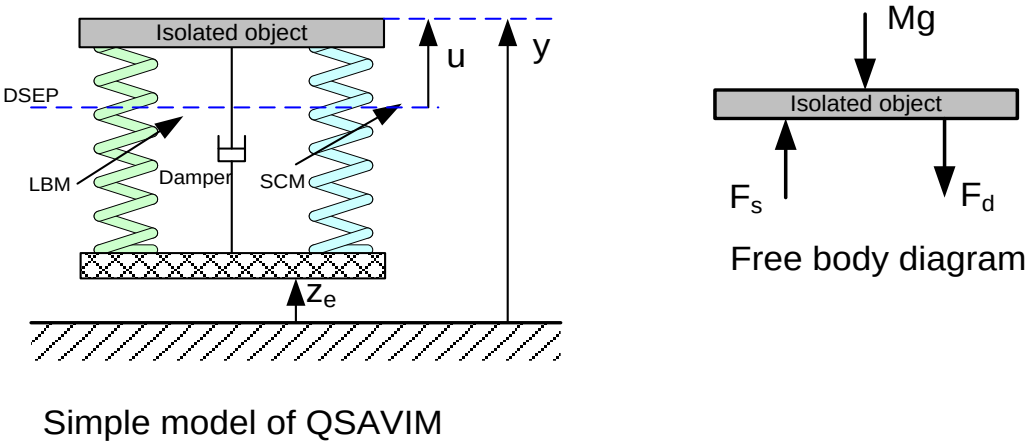

Figure.2. *Simple model of LSNVI*

The restoring force F_s [18] is expressed as following:

$$F_s = F_{LBM} + F_{SCM} \tag{1}$$

with F_{LBM} and F_{SCM} are the vertical restoring forces generated by the load bearing and the stiffness corrected mechanism, respectively.

$$\begin{aligned} F_{LBM} &= 2A_1\left[P_{s1} - P_{atm}\right]\tan\alpha \\ F_{SCM} &= 2A_2\left[P_{s2} - P_{atm}\right]\frac{u}{\sqrt{\left(R+r\right)^2 - u^2}} \end{aligned} \tag{2}$$

in which

$$\begin{aligned} P_{s1} &= P_{so1}\left(\frac{A_1h_1 + V_{ac1}}{A_1h_1 + V_{ac1} - 2A_1H_o\tan\alpha + 2A_1u\tan\alpha}\right)^n \\ P_{s2} &= P_{so2}\left(\frac{A_2h_2 + V_{ac2}}{A_2h_2 + V_{ac2} + 2A_2\sqrt{\left(R+r\right)^2 - H_o^2} - 2A_2\sqrt{\left(R+r\right)^2 - u^2}}\right)^n \end{aligned} \tag{3}$$

herein, *A* is the area of the piston, V_{ac} is the volume of the auxiliary chamber, H_{o} is called the static deformation of the system and determined by the distance between the center of the roller (4) and semicircular cam (6) as the system is at the undeformed position. *h* is the working stroke length of piston, *u* is the relative displacement between the base and isolated object. P_{so} is the pressure in the cylinder at the initial position. *n* is the ratio of specific heat capacity. It is noteworthy that subscripts "1"and "2" denote for the pneumatic cylinder 1 and 2, respectively.

The dynamic stiffness of the proposed model can be obtained by taking differentiation of Eq. (1) with respect to (*u)*, we have the stiffness model expressed in terms of dimensionless form as below:

$$\hat{K}_s = 4n\frac{\hat{V}_{d1}^n\left(\hat{h}_1+\hat{V}_{ac1}\right)^n}{\left(\hat{h}_1+\hat{V}_{ac1}-2\hat{H}_o\tan\alpha+2\hat{u}\tan\alpha\right)^{n+1}}\tan^2\alpha$$
$$\left(1+\frac{\hat{u}^2}{1-\hat{u}^2}\right)+4\hat{A}^2\mu\hat{V}_{d2}^n n\frac{\hat{u}^2}{1-\hat{u}^2}\frac{\left(\hat{A}\hat{h}_2+\hat{V}_{ac2}\right)^n}{\left(\hat{A}\hat{h}_2+\hat{V}_{ac2}+2\hat{A}\sqrt{1-\hat{H}_o^2}-2\hat{A}\sqrt{1-\hat{u}^2}\right)^{n+1}} \quad (4)$$
$$+\frac{2\hat{A}}{\sqrt{1-\hat{u}^2}}\left[\hat{P}_{atm}-\mu\hat{V}_{d2}^n\left(\frac{\hat{A}\hat{h}_2+\hat{V}_{ac2}}{\hat{A}\hat{h}_2+\hat{V}_{ac2}+2\hat{A}\sqrt{1-\hat{H}_o^2}-2\hat{A}\sqrt{1-\hat{u}^2}}\right)^n\right]$$

in which

$$\hat{A}=\frac{A_2}{A_1};\ \hat{H}_o=\frac{H_o}{R+r};\ \hat{h}=\frac{h}{R+r};\hat{P}_{atm}=\frac{P_{atm}}{P_{d_1}};\ \hat{u}=\frac{u}{R+r};\ \hat{V}_{ac1}=\frac{V_{ac1}}{A_1(R+r)};\ \hat{V}_{ac2}=\frac{V_{ac2}}{A_1(R+r)};\ \mu=\frac{P_{d2}}{P_{d1}};$$
$$V_{d1}=\frac{A_1(h_1-2H_o\tan\alpha)}{V_{e01}};\hat{F}_{LBM}=\frac{F_{LBM}}{A_1P_{d1}};\ \hat{F}_{SCM}=\frac{F_{SCM}}{A_1P_{d1}};\ \hat{V}_{d2}=\frac{A_2\left(h_2-2\left(R+r-\sqrt{(R+r)^2-H_o^2}\right)\right)}{V_{e02}};$$

herein P_d is the pressure of the pneumatic cylinder at the equilibrium position.

In order to analyze the displacement transmissibility from the base to the isolated object, the approximated equation (F_{ap}) of the restoring force given by Eq. (2) can be presented by expanding Taylor series around the static equilibrium position (u=0) as below:

$$F_{ap}=F_o+a_1u+a_2u^2+a_3u^3+a_4u^4+a_5u^5+\mathrm{O}(u^6) \quad (5)$$

herein,

$$F_o=2A_1\left[P_{so1}\left(\frac{A_1h_1+V_t}{A_1h_1+V_t-2A_1H_o\tan\alpha}\right)^n-P_{atm}\right]\tan\alpha$$
$$a_n=\frac{1}{n}\left(\frac{dF_{LBM}{}^n}{du^n}+\frac{dF_{SCM}{}^n}{du^n}\right)\Bigg|_{u=0}\qquad n=1,2,3,4,5 \quad (6)$$

Figure 3 shows the comparison between the original restoring force equation given by Eq. (1) and the approximated one given by Eq. (6). It can be seen that within expected working region, the 5-oder approximated curve denoted by the dashed line is a good agreement with the original curve plotted by the solid line. Thus, the original restoring force can be replaced by the approximated equation to analyze the dynamic response of the proposed isolation model.

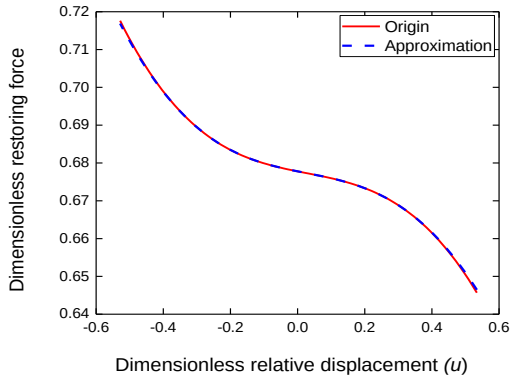

Figure 3. *Comparison between the original and approximated curve*

JTE HCMUTE
ISSN: 2615-9740
JOURNAL OF TECHNICAL EDUCATION SCIENCE
Ho Chi Minh City University of Technology and Education
Website: https://jte.hcmute.edu.vn/index.php/jte/index
Email: jte@hcmute.edu.vn

Based on free body diagram shown in Fig. 2 and applied the Newton's second law, the dynamic equation can be obtained as following:

$$M\ddot{y} + F_d - F_s + Mg = 0 \tag{7}$$

where M is the isolated object weight which is the sum of the weight of the table legs, cams, wedges and load plate, g is the acceleration of gravity, F_s is approximatively calculated by Eq. (5), F_d is the damping force calculated as below:

$$F_d = C(\dot{y} - \dot{z}_e) \tag{8}$$

with C is the damping coefficient,

The case in which the base is excited by a harmonic signal with the amplitude Z_e and frequency ω, Eq. (7) is expressed with respect to the relative displacement as following:

$$M\ddot{u} + C\dot{u} - F_{ap} + Mg = MZ_e\omega^2 \cos(\omega t) \tag{9}$$

in which $\dot{u} = (\dot{y} - \dot{z}_e)$

By letting:

$$\hat{u} = \frac{u}{Ze};\ \omega_n^2 = -\frac{1}{M}\left(\frac{dF_{LBM}}{du^n} + \frac{dF_{SCM}}{du^n}\right)\Bigg|_{u=0};$$

$$\Omega = \frac{\omega}{\omega_n};\ \tau = \omega_n t;\ \xi = \frac{C}{2\omega_n M}$$

$$\alpha_n = -\frac{1}{n!\omega_n M}\left(\frac{dF_{LBM}{}^n}{du^n} + \frac{dF_{SCM}{}^n}{du^n}\right)\Bigg|_{u=0};\ M = \frac{F_o}{g}$$

Eq. (8) can be rewritten in terms of non-dimension form as below:

$$\ddot{\hat{u}} + 2\xi\omega_n\dot{\hat{u}} + \omega_n^2\hat{u} + \sum_{n=2}^{5}\alpha_n\hat{u}^n = \omega^2\cos(\omega t) \tag{10}$$

Eq. (9) can be rearranged as:

$$\ddot{\hat{u}} + \omega_n^2\hat{u} + \varepsilon g(\hat{u},\dot{\hat{u}}) = \varepsilon k\omega^2\cos(\omega t) \tag{11}$$

herein,

$$g(\hat{u},\hat{u}) = \mu\dot{\hat{u}} + \sum_{n=2}^{5}\alpha_n^*\hat{u}^n \text{ with}$$

$$\mu = 2\xi^*\omega_n / \varepsilon;\ \alpha_n^* = \alpha_n / \varepsilon;\ k = 1/\varepsilon$$

Instead of using the frequency of the excitation ω as a parameter, a detuning parameter, describing the difference between the natural and excited frequency as below:

$$\omega_n^2 = \omega^2 - \varepsilon\sigma \tag{12}$$

By using Multi-scale method, the time scale is set to $T_i = \varepsilon^i\tau$ $(i = 0,1,2,...)$, the solution of Eq. (11) as following:

$$\hat{u}(t) = \hat{u}_o(T_o,T_1) + \varepsilon\hat{u}_1(T_o,T_1) + \varepsilon^2\hat{u}_2(T_o,T_1) + ... \tag{13}$$

and

$$\frac{d(\bullet)}{dt} = \sum_{i=0}\varepsilon^i D_i;\ \frac{d^2(\bullet)}{dt^2} = \left(\sum_{i=0}\varepsilon^i D_i\right)^2;\ \text{where } D_i = \frac{\partial(\bullet)}{dT_i}\ \ i=1,2,\ldots$$

Substituting Eqs. (12-13) into Eq. (11), then collecting the coefficients of ε^n, we have:

$$\begin{aligned}
&\varepsilon^o \quad \mathrm{D}_o^2\hat{u}_o + \omega_n^2\hat{u}_o = 0 \\
&\varepsilon^1 \quad \mathrm{D}_o^2\hat{u}_1 + \omega_n^2\hat{u}_1 = -2D_oD_1\hat{u}_o - \mu D_o\hat{u}_o - \sum_{n=2}^{5}\alpha_n^*\hat{u}^n \\
&\qquad\qquad + \sigma\hat{u}_o + \frac{k\omega^2}{2}e^{i\omega t} + c.c., \\
&\ldots
\end{aligned} \tag{14}$$

where c.c. is the conjugate term

The general solution of the first equation in Eq. (14) is expressed as below:

$$\hat{u}_o = \hat{A}e^{i\omega_n T_o} + \bar{\hat{A}}e^{-i\omega_n T_o} \tag{15}$$

with $\hat{A}$ is an unknown complex function whiles $\bar{\hat{A}}$ is the complex conjugate of *A*

The second equation of Eq. (14) is rewritten by:

$$\mathrm{D}_o^2\hat{u}_1 + \omega_n^2\hat{u}_1 = \begin{pmatrix} -2iD_1\hat{A}\omega - i\mu\hat{A}\omega \\ -\left(3\alpha_3^*\hat{A}^2\bar{\hat{A}} + 10\alpha_5^*\hat{A}^3\bar{\hat{A}}^2\right) \\ +\sigma A + \dfrac{k\omega^2}{2} \end{pmatrix} e^{i\omega t} + c.c., + \ldots \tag{16}$$

The secular terms in Eq. (16) will be ignored if the coefficient of e^{iT_o} is equal to zero, we have:

$$\begin{aligned}
&-2iD_1\hat{A}\omega - i\mu\hat{A}\omega - \left(3\alpha_3^*\hat{A}^2\bar{\hat{A}} + 10\alpha_5^*\hat{A}^3\bar{\hat{A}}^2\right) \\
&+\sigma A + \frac{k\omega^2}{2} = 0
\end{aligned} \tag{17}$$

As known, the complex function A comprising the amplitude and phase can be written as below:

$$\hat{A} = \frac{1}{2}\hat{a}e^{i\beta} \tag{18}$$

Substituting Eq. (18) into Eq. (17), then, multiplying both sides of Eq. (17) for $e^{-i\beta}$, it is obtained as:

$$\begin{aligned}
&-iD_1\hat{a}\omega + \hat{a}D_1\beta\omega - \frac{1}{2}i\mu\omega\hat{a} - \left(3\alpha_3^*\frac{\hat{a}^3}{2^3} + 10\alpha_5^*\frac{\hat{a}^5}{2^5}\right) \\
&+\sigma\frac{\hat{a}}{2} + \frac{k\omega^2}{2}\left(\cos\beta - i\sin\beta\right) = 0
\end{aligned} \tag{19}$$

Then separating the real and imaginary parts, the differential equation for amplitude and frequency of Eq. (19) is attained:

$$\begin{aligned}
&D_1\hat{a} = -\frac{1}{2}\mu\hat{a} - \frac{k\omega}{2}\sin\beta \\
&\hat{a}D_1\beta\omega = \left(3\alpha_3^*\frac{\hat{a}^3}{2^3} - 10\alpha_5^*\frac{\hat{a}^5}{2^5}\right) - \sigma\frac{\hat{a}}{2} - \frac{k\omega^2}{2}\cos\beta
\end{aligned} \tag{20}$$

The differential equation of the amplitude and phase is:

JTE
HCMUTE
ISSN: 2615-9740

JOURNAL OF TECHNICAL EDUCATION SCIENCE
Ho Chi Minh City University of Technology and Education
Website: https://jte.hcmute.edu.vn/index.php/jte/index
Email: jte@hcmute.edu.vn

$$\frac{d\hat{a}}{dt} = \varepsilon D_1 a + \mathcal{O}(\varepsilon) = -\frac{1}{2} 2\xi\omega_n \hat{a} - \frac{\omega}{2}\sin\beta$$
$$\hat{a}\frac{d\beta}{dt}\omega = \varepsilon\hat{a}D_1\beta\omega + \mathcal{O}(\varepsilon) = \left(3\alpha_3 \frac{\hat{a}^3}{2^3} - 10\alpha_5 \frac{\hat{a}^5}{2^5}\right) - \varepsilon\sigma\frac{\hat{a}}{2} - \frac{\omega^2}{2}\cos\beta \quad (21)$$

The relationship between the amplitude and phase for the relative motion (u) as the amplitude and phase are unchanged is expressed as following:

$$\left(\frac{\omega^2}{2}\right)^2 = \left(\frac{1}{2}2\xi\omega_n\omega\hat{a}\right)^2 + \left(Q - \varepsilon\sigma\frac{\hat{a}}{2}\right)^2$$
$$with\ Q = \left(3\alpha_3 \frac{\hat{a}^3}{2^3} - 10\alpha_5 \frac{\hat{a}^5}{2^5}\right) \quad (22)$$

Or:

$$\left(\hat{a}^2 - 1\right)\omega^4 - \left(2\left(\omega_n\hat{a}\right)^2 + 4Q\hat{a} - \left(2\xi\omega_n\hat{a}\right)^2\right)\omega^2$$
$$+\omega_n^4\hat{a}^2 + 4Q^2 - 4Q\hat{a}\omega_n^2 = 0 \quad (23)$$

The absolute displacement transmissibility of the LSNVI is defined as below:

$$T = \frac{Y}{Z_e} = \sqrt{\hat{a} + 1 + 2\hat{a}\cos\beta} \quad (24)$$

where, Y is the absolute vibration amplitude of the isolated object, Ze is the excited amplitude, $\hat{a}$ and β are calculated by Eq. (20) by setting $d\hat{a}/dt = 0$ and $d\beta/dt = 0$

4. Simulation results

In order to investigate the isolation effectiveness of preventing the displacement transmissibility from the base to the isolated object, the parameters of the LSNVI are set including: A_1=9.5mm^2; A_2=2mm^2; α=20^0; R=60mm; r=20mm; Ho=40mm, h=150mm; P_{d1}=2 bar, Z_e=10mm meanwhile the air pressure in the cylinder 2 is calculated by $P_{d2}=\mu P_{d1}$. The result is that the dynamic stiffness curves of the LSNVI for varied values of the pressure ratio (μ) are shown in Fig. 4 (detailed annotation of line types is given in panel of the figure). It is interesting to observe that in expected working region, the designed isolator offers the dynamic stiffness lower than the nonlinear vibration isolator without the SCM (shortened NVI non SCM). Especially, the stiffness will be increased according to the growing of the pressure ratio.

Based on these results, the transmissibility of absolute displacement is simulated by using Eq. (24) as shown in Fig. 5 (the notation of line types is presented in right-corner panel of figure). It is noteworthy that the lower stiffness is, the better isolation effectiveness of the LSNVI is. Indeed, if the μ=1.165, the stiffness of the system is the lowest (as denoted in Fig. (4), the isolation region of the LSNVI is larger than the two remaining cases of μ=1.140 and 1.100. Furthermore, it can also be seen that the resonance peak is reduced while the vibration attenuation rate is increased in accordance with the increase in the pressure ratio. Additionally, comparing with the NVI non SCM, it reveals that the LSNVI can prevent vibration transmission from the base to the isolated object better than the NVI non SCM.

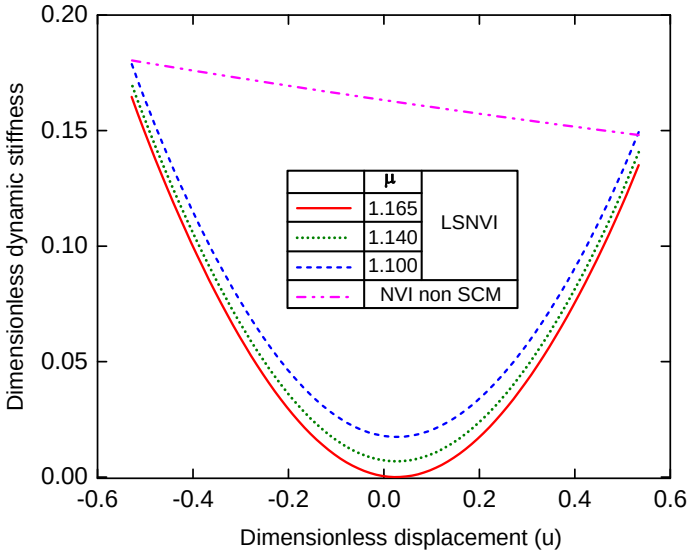

Figure.4. *Dynamic stiffness curves for various values of the pressure ratio μ*

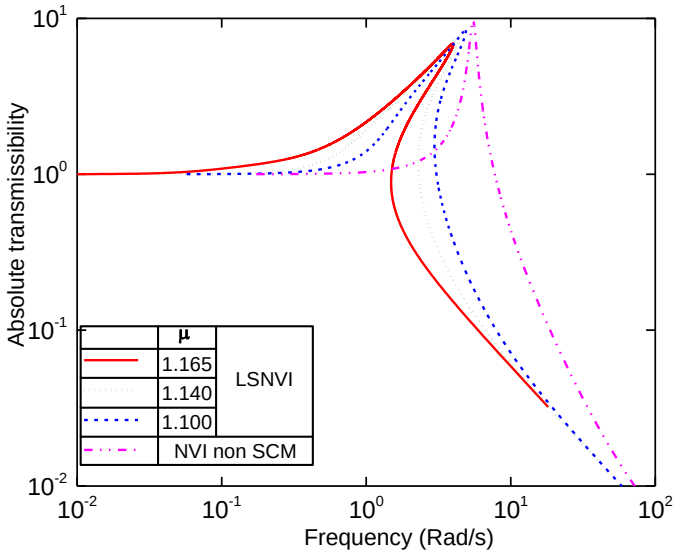

Figure.5. *Vibration transmissibility curve of the LSNVI and NVI non-SCM*

5. Conclusions

The low stiffness nonlinear vibration isolator featuring pneumatic cylinder as an elastic element was introduced in this paper. The dynamic stiffness of the isolation model was expressed and numerically calculated. The numerical simulation indicates that the stiffness can be reduced according to increasing the pressure ratio. As intruding the SCM, the stiffness of the LSNVI can be much lower than the case in which the SCM is removed.

Then, the spring force curve was approximated through expanding Taylor series to order-5. By using Multi-scale method, the primary frequency-amplitude relation of the LSNVI was then analyzed in detail. Simultaneously, the displacement transmissibility was also drawn. The simulation results indicated that the system with a lower stiffness will offer the better isolation effectiveness. In addition, the result shown that the advantages of the LSNVI against the NVI non SCM

Acknowledgments

This research is funded by Vietnam National Foundation for Science and Technology Development (NAFOSTED) under grant number 107.01-2020.36.

REFERENCES

[1] C. Wogerer , G. Nittmann and T. Panner, "Isolation of small coil spring," *IEEE International Symposium on Assembly and Manufacturing*, 2007, pp. 130-134.
[2] S.G. Kelley, *Fundamental of mechanical vibrations*, New York, McCraw-Hill, 2002.
[3] E.J. Chin, K.T. Lee, J. Winterflood, L. Ju and D.G. Blair, "Low frequency vertical geometric anti-spring vibration isolators," *Physics letters A*, vol.336, no. 2-3, pp. 97 – 105, 2005.
[4] J. Winterflood, D.G. Blair, and B. Slagmolen, "High performance vibration isolation using springs in Euler column buckling mode," *Physics Letters A*, vol.300, pp.122–130, 2002.
[5] W. Wu, X. Chen and Y. Shan, "Analysis and experiment of a vibration isolator using a novel magnetic spring with negative stiffness," *Journal of Sound and Vibration*, vol.333, pp. 2958-2970, 2014.
[6] B. Yan, H. Ma, C. Zhao, C. Wu, K. Wang and P. Wang, "A Vari-stiffness nonlinear isolator with magnetic effects: Theoretical modeling and experimental verification," *International Journal of mechanical and Sciences*, vol.148, pp.745-775, 2018
[7] A. Carrella, M.J. Brennan, T. P. Waters and K. Shin, "On the design of a high-static–low-dynamic stiffness isolator using linear mechanical springs and magnets," *Journal of Sound and vibration*, vol.315, pp. 712-720, 2008.
[8] Y. Zheng, Q. Li, B. Yan, Y. Lu and X. Zheng, "A stewart isolator with high-static–low-dynamic stiffness struts based on negative stiffness magnetic springs," *Journal of Sound and vibration*, vol.422, pp.390-408, 2018.
[9] G. Dong, X. Zhang, Y. Luo, Y. Zhang and S. Xie, "Analytical study of the low frequency multi-direction isolator with high-static-low-dynamic stiffness struts and spatial pendulum," *Mechanical Systems and Signal Processing*, vol.110, pp.521–539, 2018.
[10] G. Dong, X. Zhang, Y. Luo, Y. Zhang, and S. Xie, "Analytical study of the low frequency multi-direction isolator with high-static-low-dynamic stiffness struts and spatial pendulum," *Journal of Mechanical Systems and Signal Processing*, Vol.110, pp.521–539, 2018.
[11] M.W. Holtz and J.L.V. Niekerk, "Modeling and design of a novel air-spring for a suspension seat," *Journal of Sound and vibration*, vol.329, pp.4354-4366, 2010.
[12] I. Maciejewski, L. Meyer and T. Krzyzybski, "The vibration damping effectiveness of an active seat suspension system and its robustness to varying mass loading," *Journal of Sound and vibration*, vol.329, pp.3898-3914, 2010.
[13] I. Maciejewski, "Control system design of active seat suspension," *Journal of Sound and vibration*, vol.331, pp.1291-1309, 2012.
[14] M.M. Moheyeldein, A.M. Abd-El-Tawwab, K.A. Abd El-gwwad band M.M.M Salem, "An analystical study of the performance indices of air spring suspensions over the passive suspension," *Beni-Suef University Journal of Basic and Applied Sciences*, vol.7, pp.525-534, 2018.
[15] I. Maciejewski, S. Glowinski and T. Krzyzybski, "Active control of a seat suspension with the system adaptation to varying load mass," *Mechatronics*, vol.24, pp.1242-1253, 2014.
[16] X. B. Tran, V. L. Nguyen, and K.D.Tran, "Effects of friction models on simulation of pneumatic cylinder," *Mechanical Science*, vol.10, pp.517–528, 2019.
[17] C. H. Nguyen, C. M. Ho and K. K. Ahn, "An Air Spring Vibration Isolator Based on a Negative-Stiffness Structure for Vehicle Seat," *Journal of Applied Science*, vol.11, 2021.
[18] N.Y.P. Vo and T.D. Le, "Static analysis of low frequency isolation model using pneumatic cylinder with auxiliary chamber," *International Journal of Precision Engineering and Manufacturing*, vol.21, pp.681-697, 2020.

Nguyen Minh Ky. He received the B.S degree Mechanical engineering from Nha Trang University in 2001. In 2005, he took Ms degree from Ho Chi Minh City University of Technology. Then. He completed the Phd degree in Mechanical engineering from Ulsan University, South Korea, in 2014. His major includes nonlinear dynamic, fracture mechanics.

Vo Ngoc Yen Phuong. She completed the B.S an Ms degree in Mechanical engineering from Ho Chi Minh City University of Technology and Education and Ho Chi Minh City University of Technology in 2006 and 2010, respectively. Currently, she is a Phd student at the Mechanical engineering from Ho Chi Minh City University of Technology. Her research field includes low frequency vibration, vibration isolation

Le Thanh Danh. He received the B.S and M.S in Mechanical engineering from in Ho Chi Minh City University of Technology in 2001 and 2004. He completed and took the Phd degree in Mechanical engineering from Ulsan University, South Korea, in 2014. He is interesting in vibration isolation, nonlinear dynamic, nonlinear system control